ACES Asian Chemical Editorial Society

doi.org/10.1002/cnma.202400549

CHEMNANOMAT
Research Article

www.chemnanomat.org

Microfluidic Generation of Calcium Alginate Hydrogel Beads using External Gelation for Microalgae Cultivation

Du Tuan Tran,[a] Fariba Malekpour Galogahi,[a] Nhat-Khuong Nguyen,[a] Uditha Roshan,[a] Ajeet Singh Yadav,[a] Kamalalayam Rajan Sreejith,[a] and Nam-Trung Nguyen*[a]

Calcium alginate hydrogel beads are spherical polymeric particles with highly crosslinked network structures, known for their excellent monodispersity and retention capabilities. These beads, produced by high-throughput droplet-based microfluidic techniques, are widely used for encapsulating and cultivating various microscopic particles such as cells. While internal gelation has been commonly utilized for crosslinking of calcium alginate hydrogel beads in microalgae encapsulation, the use of external gelation remains underexplored. This study utilized droplet-based microfluidic technology combined with external gelation to produce calcium alginate hydrogel beads for encapsulating the microalgal strain *Chlorella vulgaris*. Emulsions containing emulsified calcium ions served as the crosslinking phase. Initial geometrical analysis indicated that beads crosslinked with a high concentration of calcium ions (1 g/mL) achieve superior size uniformity and shape consistency. Microalgae cultivation experiments using these beads demonstrated steady growth of *Chlorella vulgaris* over a 5-day period, with the beads maintaining their geometric stability until the final day when minor cell leakage was observed. These results provide a foundation for future molecular-level studies on microalgae cultivation in hydrogel beads and suggest potential applications in fields requiring precisely controlled microalgae growth.

1. Introduction

Microalgae cultivation is the process of growing microalgae under controlled conditions to harness their biological and biochemical properties for various applications. This process has long been an essential technique for the rapid production of biomass such as proteins, lipids and carbohydrates derived from the microalgal cell bodies, which find applications in biofuel production, carbon sequestration, and the development of food supplements and pharmaceuticals.[1–4] Although large-scale microalgae cultivation has been implemented by many biotechnology companies for commercial purposes, fundamental research at the lab scale remains essential for optimizing and advancing cultivation technologies. The advent of microfluidic technologies has revolutionized microalgae research by miniaturizing the cultivation process to the microscale, significantly reducing the required quantities of cells, growth medium, and related nutrients.[5,6] Microscale microalgae culture offers several key advantages over conventional macroscopic methods, including higher throughput for sample preparation, improved control over cultivation conditions, and a lower risk of contamination.[7–9] Depending on the application, microfluidic devices can be designed to store and grow microalgae within their microchannels or reservoir systems, or as droplet generators to produce discrete microscale liquid droplets for microalgae encapsulation and subsequent cultivation. These adaptable designs have opened new avenues of research, allowing scientists to model and simulate complex growth environments, achieve precise control of microalgal interactions, and conduct in-depth investigations of algal growth behaviors at the single-cell level.[10–12]

Droplet-based microfluidics is an emerging microfluidics-based research area which focuses on the generation and manipulation of miniaturized liquid droplets. The high-throughput generation process of monodisperse droplets takes place inside microfluidic devices with intricate microchannel designs, whereas droplet manipulation and handling can be carried out inside (on-chip) or outside the devices (off-chip). Typically, the preparation and controlled infusion of at least two immiscible fluids into microfluidic devices are necessary for stable droplet production. The fluids responsible for droplet formation are known as dispersed phases, while those serving as the medium for droplet dispersion are referred to as continuous phases. Comparing with other conventional droplet formation methods such as manual pipetting, emulsification or coacervation, droplet-based microfluidics offers several advantages including minimized reagent consumption, scalable automated process, excellent droplet monodispersity, and the ability to integrate other systems into a single device for further droplet manipulation.[13–15] These benefits have been leveraged for a wide range of biomedical, chemical, and environmental applications, including micro-reactors, drug delivery, cell culture, and digital PCR (dPCR) for DNA quantification.[16–20]

In addition to the generation of bare droplets, droplet-based microfluidics have been employed to produce miniaturized solid beads, such as hydrogel beads or microcapsules. These beads are originally polymer-based liquid droplets, which

[a] D. Tuan Tran, F. Malekpour Galogahi, N.-K. Nguyen, U. Roshan, A. Singh Yadav, K. Rajan Sreejith, N.-T. Nguyen
Queensland Micro- and Nanotechnology Centre, Griffith University, 170 Kessels Road, Nathan, QLD 4111, Australia
E-mail: nam-trung.nguyen@griffith.edu.au

are transformed into solid beads via various on-chip or off-chip solidification methods. Due to the complex formation mechanism, more than two immiscible fluids are usually required for the generation of solid beads. Biodegradable polymers, such as sodium alginate, are ideal base materials for production of polymeric solid beads due to their widespread availabilities, bio-compatibility profile and ease of processing. Sodium alginate is a popular and low-cost seaweed-based polysaccharide known for its ability to crosslink with some specific ions in aqueous media and form a hydrogel structure. This unique feature has been exploited in droplet-based microfluidics to induce effective on-chip gelation of sodium alginate droplets and production of monodisperse alginate solid beads.[21–23]

Generally, on-chip gelation of sodium alginate droplets can occur either internally (internal gelation) or externally (external gelation). Calcium ions are the most commonly used crosslinking agents, facilitating the formation of calcium alginate hydrogel beads. For internal gelation, the crosslinking ions are embedded in one of the dispersed phases and crosslinking reaction is triggered when the ions come into contact with sodium alginate. To prevent cross-junction blockages and device failures due to rapid gelation, weakly soluble calcium salts such as calcium carbonate ($CaCO_3$) or calcium-ethylenediaminetetraacetic acid (Ca-EDTA) are commonly used. These salts release crosslinking calcium ions slowly when triggered by an acidified oil phase.[22,24, 25] However, there is a high risk of channel clogging caused by precipitation of undissolved salt particles over prolonged period.[23,26, 27] External gelation is an ideal alternative method for generation of beads with minimal clogging issues. One of the most common techniques to induce external gelation is to emulsify highly water-soluble calcium salts such as calcium chloride ($CaCl_2$) in oil to yield emulsions. By introducing emulsion as the continuous phase, the emulsified calcium ions gradually migrate to the interphase and react with sodium alginate droplets, leading to gelation.[28,29] For example, Liu et al. successfully produced monodisperse calcium alginate hydrogel beads using $CaCl_2$ emulsion based on corn oil as the crosslinking continuous phase. Despite the presence of magnetic particles in the sodium alginate droplets, calcium ions were still able to penetrate inside the droplets and induce gelation to form hydrogel beads with desired magneto-responsive properties.[30] External gelation has also been demonstrated as a bio-friendly method for cell encapsulation applications. For example, Agarwal et al. utilised a non-planar microfluidic device coupled with external gelation technique to generate core-shell alginate beads with collagen core for encapsulation and culture of stem cells. This distinct core-shell structure allows for precise control over cell and tissue proliferation, adhesion, and differentiation by modifying the extracellular matrix (ECM) properties of the core, which can be beneficial for a wide range of biomedical applications.[31]

To the best of our knowledge, no previous studies have explored the encapsulation of microalgae within calcium alginate solid beads using the external gelation method, although this approach holds significant potential for creating a stable bead platform for microalgal cell retention and growth. Thus, in this study, we attempted to employ external gelation for generation of monodisperse calcium alginate hydrogel beads, as well as encapsulation and cultivation of microalgae inside the beads. We used soft lithography to create microfluidic devices that functioned as hydrogel bead generators. Emulsion made of $CaCl_2$ and mineral oil was prepared and used as the crosslinking phases for bead production. We investigated the effect of different concentrations of calcium ions on the generation of blank beads. For cell growth characterization, we focused on analyzing the stabilities and cell growth behaviors of the bead platforms with optimal calcium ion concentration. The successful encapsulation and cultivation of microalgae using external gelation could pave the way for future research into creating and optimizing structurally stable miniaturized platforms for microalgae research.

Experimental section

Materials and Apparatus

The base polymer and the curing agent of elastomeric polydimethylsiloxane (PDMS) was purchased from Dow Corning (MI, USA) under trade name SYLGARD™ 184. Negative epoxy-based photoresist SU-8 was purchased from Kayaku Advanced Materials, Inc. (MA, USA). Sodium alginate, calcium chloride dihydrate, mineral oil, non-ionic surfactant Span® 80, trichloro(1H,1H,2H,2H-perfluorooctyl)silane (PFOCTS) and BG-11 culture medium were acquired from Sigma-Aldrich (Merck KGaA, Germany). Commercial rain repellent agent Rain-X® Glass Treatment (ITW, IL, USA) was purchased from a local supplier. The *Chlorella vulgaris* microalgal strain, codenamed CS-41, was obtained from the Commonwealth Scientific and Industrial Research Organisation (CSIRO).

Pre-Culture of Microalgae

Chlorella vulgaris was sub-cultured in sterilized BG-11 medium in an enclosed cultivation chamber at 25 °C under LED growth light with 12 : 12 h light-dark cycle. The photosynthetic photon flux density (PPFD) of the LED growth light was set at 57 μmol/m^{2}s. After 6 days, microalgal cells were separated from the growth medium at exponential growth phase using centrifugation (4,500 rpm, 5 minutes). The centrifuged microalgae were then resuspended in Milli-Q water and ready for the encapsulation experiment.

Design of the Microfluidic Channel

The design of a photolithographic mask with a microchannel pattern was carried out using CleWin software (WieWeb software, The Netherlands). We designed a microchannel system with two connected flow-focusing cross-junctions: the first junction for the generation of sodium alginate droplets and the second junction for the crosslinking reaction of sodium alginate droplets to form calcium alginate hydrogel beads. The design includes three inlets and one outlet: inlet 1 introduces the aqueous solution (sodium alginate solution or sodium alginate-microalgae mixture), inlet 2 is for the first continuous phase (mineral oil with Span® 80 surfactant), inlet 3 serves as the second continuous phase and emulsion phase (initially mineral oil with Span® 80 surfactant, then replaced with mineral oil-calcium chloride emulsion), and the outlet is for the collection of the generated hydrogel beads. The main channel connecting the two cross-junctions has a width of 200 μm.

The first junction has a constriction area with a channel width of 50 μm. The entire microchannel system has a depth of 130 μm.

Fabrication of Flow-Focusing Microfluidic Device

The microchannel design from the photolithographic mask was transferred onto a silicon wafer using the photolithography process.[32,33] The resulting master mould with SU-8 patterned microchannels underwent silanization treatment with PFOCTS to facilitate the later removal of PDMS.

PDMS microfluidic device was fabricated using the soft lithography technique. First, the PDMS base and curing agent were mixed in a ratio of 10 to 1. After degassing in a desiccator, the mixture was poured into the master mould and cured at 80 °C in an oven for 3 hours. The PDMS slab was then peeled off from the master mould. The inlets and outlet were subsequently created using a biopsy punch. Finally, the cleaned PDMS slab was bonded to a glass slide following an oxygen plasma treatment step (PDC-32G-2, Harrick Plasma) for 120 s at 1.2 mbar.

Surface Treatment of Microfluidic Device

Hydrophobic treatment was applied to the microchannel to ensure the flow consistency of oil-based continuous phases. First, the microfluidic device was placed on a hot plate set to 150 C for 15 minutes. Next, commercial rain repellent agent Rain-X® Glass Treatment was infused into the microchannel and allowed to remain in the device for 7 mins. Finally, the residual rain-repellent agent was then blow-dried using nitrogen gas, making the treated microfluidic device ready for the hydrogel bead generation experiment.

Generation of Calcium Alginate Hydrogel Beads with and without Encapsulation of Microalgae

Prior to the main experiment, the inlet fluids were prepared and loaded into the syringes. For generation of blank /hydrogel beads, sodium alginate solution (1% w/v) was used as the dispersed phase. For hydrogel beads with encapsulated microalgae, the dispersed phase was prepared by thoroughly mixing a 2% w/w sodium alginate solution with pre-cultured microalgae stock in a 1:1 volume ratio. Meanwhile, two different continuous phases were prepared and used for the generation of both blank hydrogel beads and beads with encapsulated microalgae. The first continuous phase was created by mixing mineral oil with Span® 80 (5% w/w). The second continuous phase for crosslinking of sodium alginate and calcium chloride was prepared by mixing mineral oil (containing Span® 80 as an emulsifier) and calcium chloride solution. The concentration of Span® 80 in mineral oil was 1.25% w/w, and the ratio between aqueous solution and mineral oil was fixed at 1:5. The aqueous solution-oil mixture was thoroughly emulsified using an ultrasonic homogenizer (Vibra-Cell™ Ultrasonic Liquid Processors, Sonics & Materials Inc, CT, USA) for 1 minute to yield stable water-in-oil (W/O) emulsions.

To initiate the experiment, the microfluidic device was first placed under an inverted microscope (ECLIPSE Ti2, Nikon, Japan) with an attached high-speed camera (Chronos 2.1-HD High Speed Camera, Kron Technologies Inc., Canada) for real-time monitoring of the entire fabrication process. The inlets of the device were connected with respective syringes, while the outlet tubing was placed into a blank petri dish. The inlet fluids were introduced into the microfluidic device using a syringe pump (NEM–B101-03 A, CETONI GmbH, Germany). First, the dispersed phase was delivered into inlet 1 with a flow rate of 400 μL/hr, and mineral oil continuous phases were introduced into both inlet 2 and 3 with flow rates of 1,000 μL/hr. The emulsion phase was not introduced at this initial stage of experiment to avoid possible interaction between the emulsion and dispersed phase due to pressure imbalance. This could lead to the unwanted formation of calcium alginate gel at the first junction and eventual device blockage. After stable aqueous droplets were formed at the first junction, the mineral oil continuous phase at inlet 3 was replaced with the emulsion, which was infused into the device at the same flow rate (1,000 μL/hr) to initiate the emulsion reaction between sodium alginate droplets calcium ions in the emulsion. The outlet tubing was then placed into a centrifuge tube containing calcium chloride solution (0.05 g/mL) for collection and further crosslinking of hydrogel beads which occurs at the oil-water interface. The total collection time of the beads was fixed at 2 minutes, resulting in an estimated collection of around 300–400 beads.

Extraction and Rinsing of /Hydrogel Beads

Extraction of calcium alginate hydrogel beads into aqueous phase and subsequent rinsing of beads are required for geometrical analysis and cell growth experiments. First, the centrifuge tube with collected beads was thoroughly mixed using a vortex mixer for 5 s, and then centrifuged at 5,000 rpm for 5 mins to separate the aqueous and oil phases. The bottom aqueous phase containing the hydrogel beads was then manually extracted to a new centrifuge tube using a micropipette, followed by repeated rinsing of beads with calcium chloride solution (0.05 g/mL) until the mixture was free of residual emulsions. Finally, the cleaned calcium alginate hydrogel beads were ready for analysis and microalgae cultivation experiments.

Cultivation of Hydrogel Beads with Encapsulated Microalgae

The rinsed calcium alginate hydrogel beads were first redispersed into 100 μL sterile culture medium BG-11. Next, the mixture was transferred to a 96-well plate, which was placed inside an enclosed chamber for cultivation experiment under LED growth light with 12:12 h light-dark cycle and fixed temperature of 25 °C. The photosynthetic photon flux density (PPFD) of the LED growth light was set at 57 μmol/m^{2}s. The total cultivation time was 5 days, and hydrogel beads were monitored daily to investigate the cell behavior and any potential changes in the bead geometries. The real size and design of microfluidic devices were revealed in Figure 1a and 1b, while the schematics of calcium alginate bead generation with encapsulated microalgae was illustrated in Figure 1c.

Characterization

The images of calcium alginate and encapsulated microalgae were captured using an inverted microscope Nikon ECLIPSE Ti2 (Nikon, Japan) with integrated phase contrast and epi-fluorescence imaging. The captured images were analyzed using ImageJ freeware (NIH, USA) to extract data on bead dimensions.

Statistical Analysis

To quantify the dispersion of bead size measurements around the mean, the coefficient of variation (CV) was calculated as follows:

$$CV\ (\%) = \frac{\sigma}{\mu} \times 100 \quad (1)$$

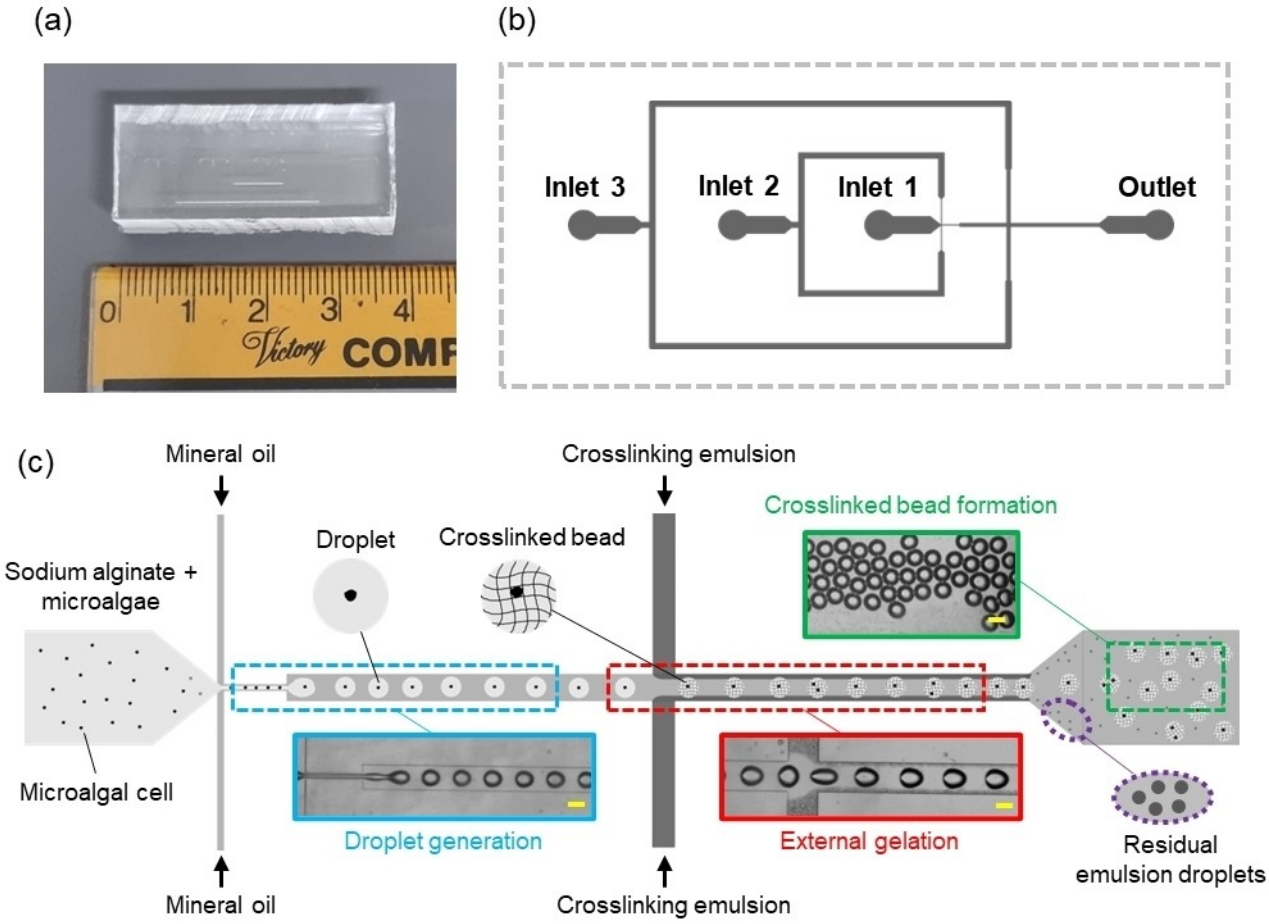

Figure 1. Microfluidic device for generation of calcium alginate hydrogel beads: (a) Real image of a microfluidic device; (b) Microchannel design with 3 inlets and 1 outlet; (c) Schematics of microfluidic generation of calcium alginate hydrogel beads with encapsulated microalgae, including droplet generation after first junction, external gelation after second junction, and formation of crosslinked beads at outlet. Scale bar represents 100 μm.

Where σ is the standard deviation (μm), and μ is the mean (μm) of the dataset.

The sphericity factor of the hydrogel beads is used as an indicator of sphericity. The equation of the sphericity factor is as follows:

$$S = \frac{d_{max} - d_{min}}{d_{max} + d_{min}} \tag{2}$$

Where d_{max} is the maximum diameter and d_{min} is the minimum diameter of the hydrogel beads.

The statistical analysis of geometries of hydrogel beads and determination of optimal microalgal cell concentration based on Poisson distribution were performed using a Python module designed for statistical functions (scipy.stats). The formula for Poisson distribution is given by:

$$p(k,\lambda) = \frac{\lambda^k e^{-\lambda}}{k!} \tag{3}$$

Where p is the probability of beads containing k cells, k is the number of individual cells in a droplet and λ is the average number of cells per droplet volume. More thoroughly, λ can be defined as the ratio between the number of microalgae cells N_{cell} and the number of droplets N_{drop} generated from a given volume of sodium alginate dispersed phase. Thus, λ can also be expressed as:

$$\lambda = \frac{N_{cell}}{N_{drop}} \tag{4}$$

Number of beads (or droplets) N_{drop} can also be defined as the ratio between the volume of pre-encapsulation solution V_{sol} and the volume of one droplet V_{drop}, assuming that all the droplets are transformed into cross-linked hydrogel beads later on without distortion in dimensions:

$$N_{drop} = \frac{V_{sol}}{V_{drop}} \tag{5}$$

The number of microalgal cells in one volume unit (cells/mL) C in pre-encapsulation sodium alginate solution can be derived by combining Equation (3) and (4), with $V_{sol} = 1$ mL, as follows:

$$C = \frac{6\lambda}{\pi {d_{drop}}^3} \times 10^{12} \tag{6}$$

Where d_{drop} is the diameter of the droplet (μm), assuming that the droplets are spherical in shape.

The encapsulation efficiency of microalgal cells within calcium alginate hydrogel beads was determined by calculating the percentage of cells successfully encapsulated inside the beads. Fluorescent images of the beads were captured immediately after collection from the device outlet using the epi-fluorescence imaging feature. These images were then analyzed using ImageJ software, and the encapsulation efficiency was calculated using the following formula:

$$E\ (\%) = \frac{T - T_0}{T} x\ 100\% \quad (7)$$

Where E is the encapsulation efficiency (%), T is the total number of cells counted in the capture image, and T_o is the total number of cells not encapsulated inside the beads.

3. Results and discussions

3.1. Generation of Calcium Alginate Hydrogel Beads with and without Encapsulated Microalgae

The concentration of calcium ions in the emulsion phase is crucial for the formation and final geometry of calcium alginate hydrogel beads. Selecting the optimal calcium ion concentration is essential for generating monodisperse and dimensionally stable hydrogel beads, which ensures consistent microalgae encapsulation, facilitates controlled cultivation, and simplifies growth characterization. While previous studies have determined optimal calcium ion concentrations in microfluidic settings, it remains necessary to conduct this analysis due to variations in microfluidic device designs, fluid component compositions, and environmental factors. In this study, besides varying calcium ion concentration in the emulsion phase, we also prepared both blank calcium alginate hydrogel beads and beads with encapsulated microalgae to understand the potential influences of microalgae presence in the dispersed phase on the resulting bead geometries. The cell number in the alginate dispersed phase and the flow rates of all fluid phases were kept constant. The initial cell number was determined using the Poisson distribution to maximize the number of beads containing a single cell, enabling clear observation of cell growth in subsequent microscopic analyses. According to Equations (1), (2), (3) and (4), the probability of droplets p containing k cells is governed by controllable factors such as cell number per unit of volume C and the diameter of the droplet d_{drop}, and is independent of the size of encapsulation contents. Cell number per unit of volume C is determined prior to the preparation of the pre-encapsulation solution, while d_{drop} can be controlled using device channel geometries and flow rates of input liquids. Through the representation of Poisson distribution, Collins et al. revealed that the encapsulation probability of single-cell ($k = 1$) in droplets is maximized when $\lambda = 1$.[34] Given that the microchannel in this study was designed to produce hydrogel beads with 100 ± 20 μm in size, the calculated optimal cell number for single-cell encapsulation falls ranges from 1.1 x 10^6 cells.mL^{-1} to 3.7 x 10^6 cells/mL^{-1}. To ensure the pre-encapsulation solution of microalgae falls within the calculated range, we determined the actual cell concentration in the microalgae culture stocks from the pre-culture process using a cell counting technique before performing subsequent dilutions with sodium alginate solution to adjust the concentration to the desired value. The cell counting process involved utilizing a hemocytometer (for cell holding), an inverted microscope (for cell observation), and image analysis (to obtain the final cell count).

Figure 2 represents the geometrical analysis of calcium alginate hydrogel beads with and without encapsulated microalgae based on maximum diameter and percentage of highly spherical beads. We used the maximum diameter for dimensional comparison rather than the mean diameter due to the presence of a considerable number of non-spherical and oval-shaped beads across all platforms. The maximum diameter provides a more accurate comparison of size distributions between beads formed at different crosslinked calcium ion concentrations. To compare sphericity, we calculated the sphericity of each bead using Equation (2) and determined the proportion of highly spherical beads for each calcium ion concentration by dividing the number of beads with sphericities below 0.05 by the total number of beads. This method simplifies sphericity comparison into a single, convenient value rather than comparing widely distributed individual sphericities. The microscopic images indicate the overall trend of increasing uniformities of bead size with increasing calcium ion concentrations for both types of hydrogel beads. The maximum calcium ion concentration was capped at 1 g/mL due to incomplete dissolution of calcium salts at higher concentrations based on our observations. The corresponding histograms support this observation, showing narrower bead size distributions and a decreasing coefficient of variation (CV) at higher calcium ion concentrations (particularly at 1 g/mL), which indicates superior monodispersity. with a variety of sizes and shapes tend to aggregate and form hydrogel clumps. At lower calcium ion concentrations, deformed hydrogel beads of varying sizes and shapes tend to aggregate, forming clumps. This is likely due to incomplete gelation of alginate droplets caused by insufficient calcium ions in the emulsion phase, leading to deformation and merging of droplets upon interaction at downstream.[28] This explanation also aligns with the sphericity characterization, where the beads formed with the highest calcium ion concentration (1 g/mL) stood out from the others with a significantly higher percentage of highly spherical beads.

As shown in Figure 2a and 2b, the encapsulation of microalgae in the disperse phase appeared to enlarge the alginate droplets, resulting in slightly larger beads containing microalgae compared to the blank beads. Interestingly, this increase in size had a positive impact only on the beads with the highest concentration of calcium ions (1 g/mL), as evidenced by a lower CV and a higher percentage of highly spherical beads. The increase in viscosity could be a contributing factor that enhances the stability of the alginate droplets, leading to improved monodispersity and a greater number of highly spherical hydrogel beads.[35] On the other hand, conflicting effects of microalgae encapsulation were observed in other

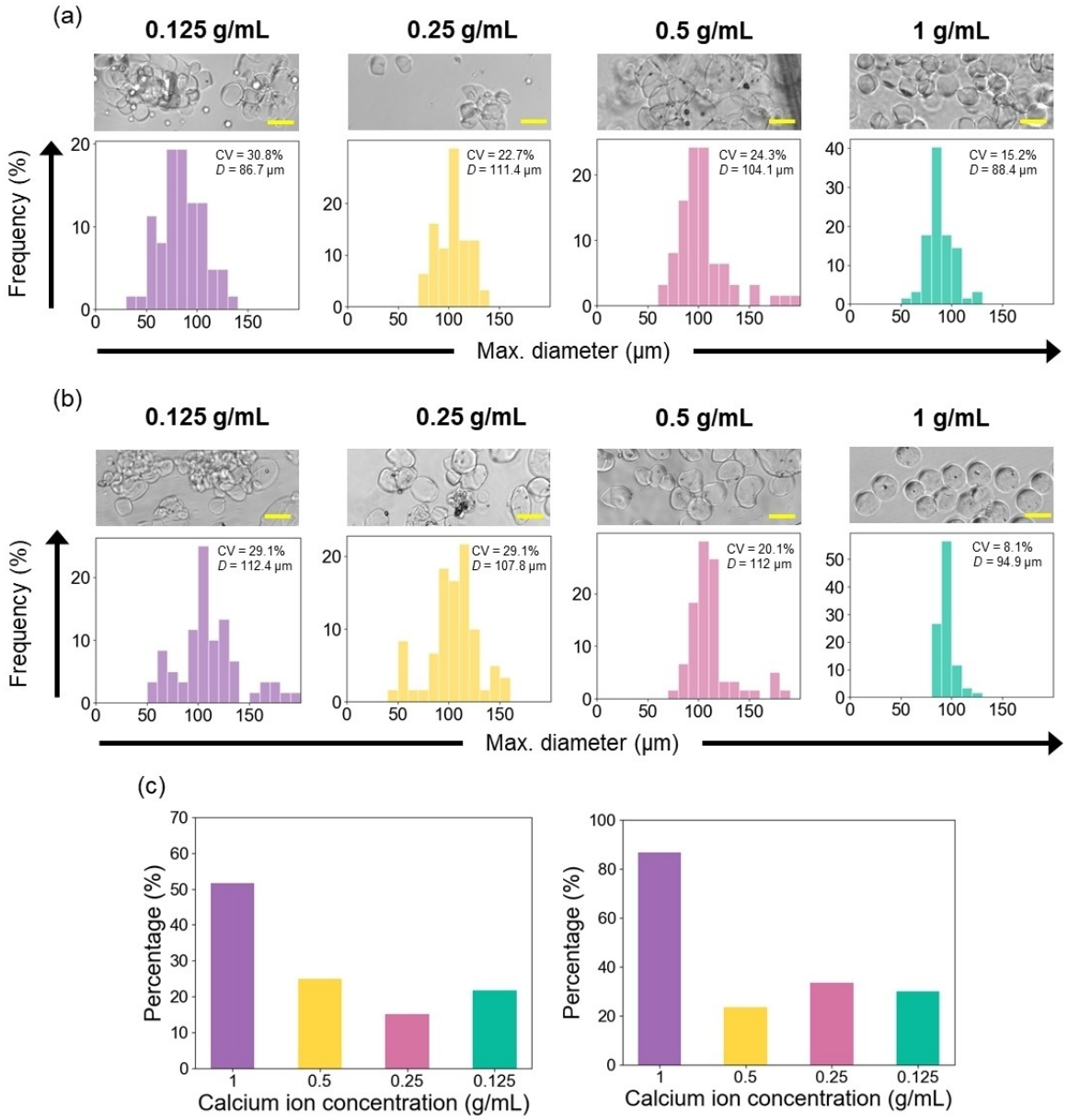

Figure 2. Geometrical analysis of calcium alginate hydrogel beads crosslinked by varying calcium ion concentrations, with and without encapsulation of microalgae: Microscopic images accompanied by bead size distribution of (a) blank beads and (b) beads with encapsulated microalgae; (c) Proportions of blank beads (left) and beads with encapsulated microalgae (right) that are highly spherical (sphericity $S < 0.05$). Value D indicates the average of the maximum diameters. Scale bars represent 100 μm.

bead platforms, likely due to incomplete gelation issues that undermined the stabilizing effect of the increased droplet viscosity.

3.2. Cultivation of Microalgae in Calcium Alginate Hydrogel Beads

In this section, we focused on the characterization of microalgae growth within calcium alginate hydrogel beads reinforced with the highest calcium ion concentration (1 g/mL), identified as the optimal platform for cell cultivation. Before analyzing cell growth, we calculated the encapsulation efficiency using Equation 7. The results showed an efficiency of 99.65 ± 1.36%, highlighting the critical role of the high calcium ion concentration (1 g/mL) in reinforcing the beads and preventing microalgal cell leakage during and after the microfluidic generation process. The high encapsulation efficiency also ensures a reliable starting point for assessing microalgal growth within the beads during the cultivation experiment. As mentioned earlier, other bead platforms showed inconsistent bead formation, suggesting potential structural instabilities that could affect cell growth. To evaluate cell growth efficiency during the cultivation period, we employed bright-field and fluorescence microscopy to observe microalgae encapsulated within the calcium alginate hydrogel beads. For bright-field

imaging, we used a phase contrast technique integrated with the microscope to achieve a clear contrast between the beads and the background. Fluorescence images were simultaneously captured using the epi-fluorescence technique to locate the cells based on their emitted fluorescence signals. An excitation light source with a wavelength of 490 nm was used to induce the autofluorescence of chlorophyll molecules within the microalgal cells, resulting in red fluorescence emission.[36–38]

Figure 3 shows a general increase in cell numbers and the formation of multi-celled beads (beads containing at least two cells), confirming the ability of microalgal cells to grow within calcium alginate hydrogels over the 5-day cultivation period. This result demonstrates the mechanical resilience of Chlorella vulgaris cells, which were able to survive the bead fabrication and extraction processes, and their tolerance to oil, given the possibility of trace amounts of emulsion residues in the growth medium.[39] On the first day of cultivation, the numbers of blank beads, single-cell beads, and multi-cell beads were almost equal. By day 3, cell proliferation and division became evident, as indicated by the predominance of multi-cell beads. By day 5, many cell clusters had formed due to the aggregation of newly divided cells with the original ones. We also observed cell leakage from the hydrogel beads and external cell growth outside the beads. This likely resulted from the swelling of hydrogel beads combined with the rapid growth of cells near the bead boundaries, which allowed newly grown cells to penetrate and migrate into the surrounding growth medium.[40–42] This explanation agrees with the observed distortion of bead shapes, particularly noticeable on day 5, indicating potential structural changes in the hydrogel beads.

3.3. Geometrical Stabilities of Calcium Alginate Hydrogel Beads

In this section, we conducted a detailed geometrical analysis to assess the significance of changes in bead geometry during the cultivation period. Similar to the approach in Section 3.1, maximum diameters of the beads were used for this analysis. The histograms in Figure 4a show that the geometries of the hydrogel beads remained relatively stable over the first three days of cultivation, as indicated by the similar coefficients of variation (CVs) between these days. However, a decline in bead size uniformity is evident on the final day of the experiment, with a moderate increase in CVs. This can be attributed to the distortion of bead shapes over the cultivation period. Figure 4b illustrates the typical appearances of highly spherical hydrogel beads and severely distorted, non-spherical beads. The declining stability in bead shapes is confirmed by Figure 4c, which shows a general decrease in the number of highly spherical beads. These analytical results are consistent with the microscopic observations discussed in the previous section, where shape distortions were evident in the images from day 5. The swelling of hydrogel beads when immersed in an aqueous medium and the ion exchange process are likely the primary factors contributing to these unfavorable geometric changes. Variations in the degree of swelling among the beads result in differences in bead sizes, distortions in shape, and a general decline in uniformity. Additionally, the presence of monovalent ions in the BG-11 medium may cause a gradual ion exchange between the growth medium and the hydrogel beads, leading to the loss of calcium ions from the beads and their structural weakening over time.[43]

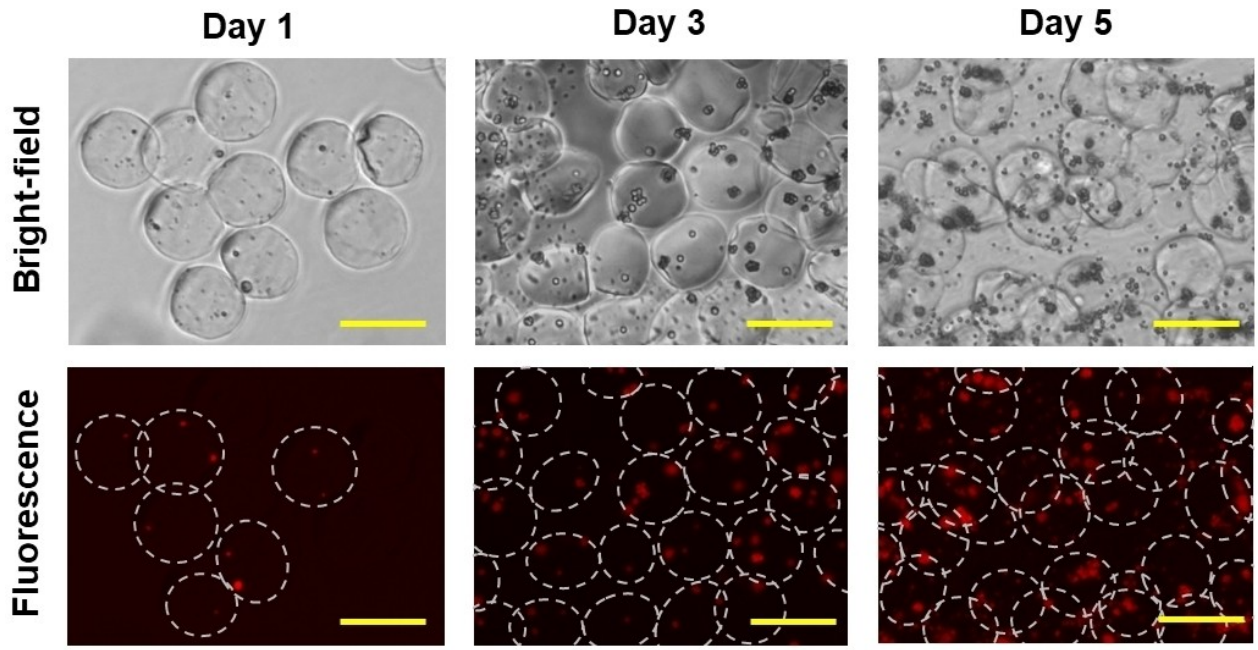

Figure 3. Growth of microalgal cells within calcium alginate hydrogel beads (calcium ion concentration 1 g/mL) over a 5-day period, as observed in microscopic bright-field and fluorescence images. In the fluorescence images, the boundaries of beads containing encapsulated microalgal cells are marked with white dashed circles. Scale bars indicate 100 μm.

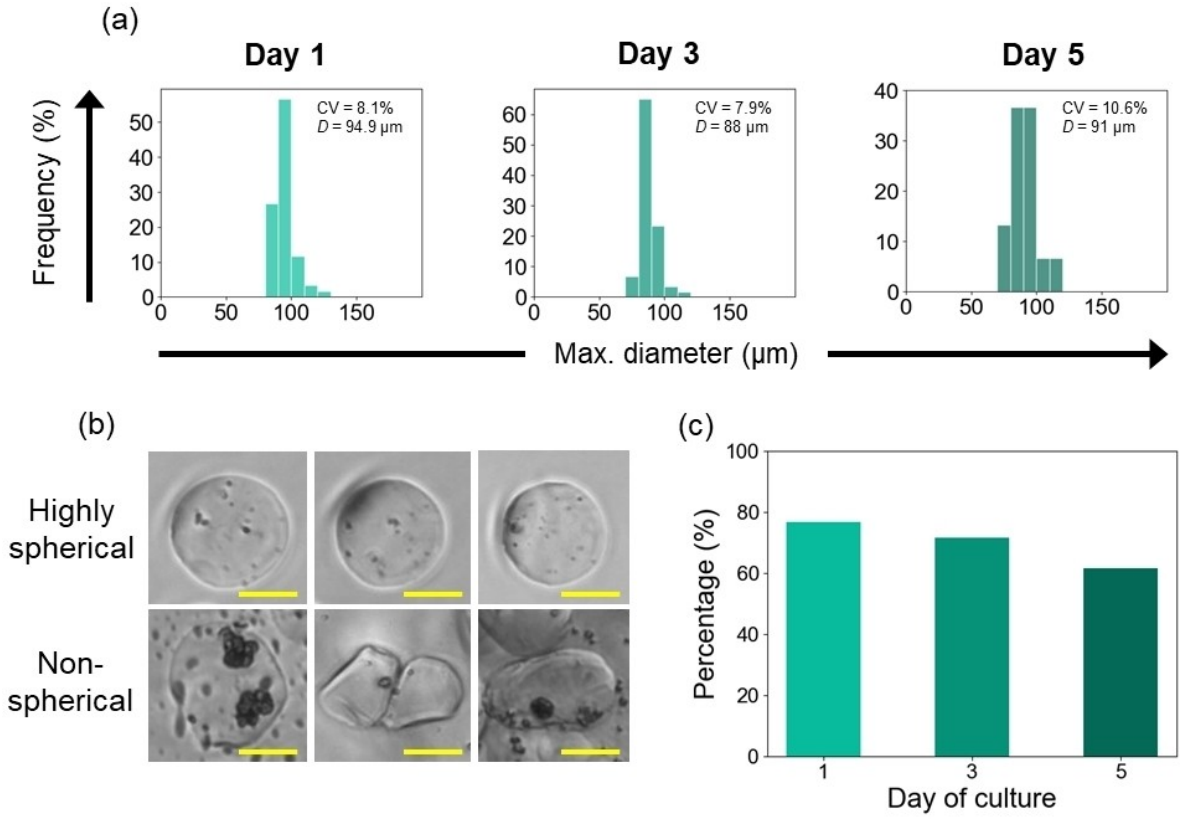

Figure 4. Geometrical changes of calcium alginate hydrogel beads over 5-day cultivation period: (a) Bead size distribution during the cultivation period; (b) Microscopic images of typical highly spherical and non-spherical beads; (c) Proportions of hydrogel beads that are highly spherical (sphericity S $<$ 0.05). Maximum Value D indicates the average of the maximum diameters. Scale bars indicate 50 μm.

4. Conclusions

In this study, we successfully developed a straightforward method for fabricating calcium alginate hydrogel beads and encapsulating microalgae *Chlorella vulgaris* within these beads. For the high-throughput production of monodisperse hydrogel beads, we employed a simple flow-focusing microfluidic device with two cross-junctions: the first for forming alginate droplets and the second for converting these droplets into crosslinked hydrogel beads through external gelation with emulsified calcium ions. The initial geometrical analysis demonstrated that calcium alginate hydrogel beads crosslinked with the highest calcium ion concentration (1 g/mL) possessed superior size uniformity and sphericity. We used these optimal beads for the main microalgae cultivation experiment, where microscopic observations indicated that microalgal cells grew healthily and formed clusters inside the hydrogel beads. However, some cell leakage into the surrounding growth medium was observed on the final day of cultivation. Geometrical analysis revealed that the beads maintained structural resilience and excellentsize uniformity after three days of cultivation. By the final day, bead shape distortion and a decline in size uniformity were noted, correlating with the observed cell leakage. The results of this study provide a solid foundation for future research on microalgae cultivation within miniaturized, biocompatible hydrogel beads produced via microfluidic technologies, particularly those utilizing external gelation for bead formation. Future research will first focus on addressing the issue of cell leakage by enhancing the mechanical integrity and swelling resistance of calcium alginate hydrogel beads, thereby enabling extended cell analysis beyond the current cultivation period of five days. Further studies could investigate microalgal cell processing related to single-cell analysis, such as isolating and cultivating single-cell beads to evaluate valuable biomass components like proteins and lipids and identifying microalgae strains with superior growth characteristics. Additionally, the microalgae within the calcium alginate hydrogel beads can be possibly recovered by dissolving the beads with chelating agents such as sodium citrate or sodium calcium edetate (calcium EDTA), facilitating potential cell repurposing applications.

Acknowledgements

N. T. N. acknowledges funding support from Australian Research Council through the Australian Laureate Fellowship (FL230100023) and the Discovery Project (DP220100261). D.T.T. acknowledges tuition fee offset support from Commonwealth Government through the Australian Government Research Training Program Scholarship. The photolithography process was carried out at the NCRIS-enabled Australian National Fabrication Facility, Queensland node (ANFF–Q), Griffith Hub.

Open Access publishing facilitated by Griffith University, as part of the Wiley - Griffith University agreement via the Council of Australian University Librarians.

Conflict of Interests

The authors declare no conflict of interest.

Data Availability Statement

The data that support the findings of this study are available from the corresponding author upon reasonable request.

Keywords: calcium alginate · hydrogel beads · microalgae · external gelation · flow-focusing microfluidic devices · emulsified calcium ions · structural stability

[1] S. Kandasamy, B. Zhang, Z. He, N. Bhuvanendran, A. I. El-Seesy, Q. Wang, M. Narayanan, P. Thangavel, M. A. Dar, *Fuel* **2022**, *308*, 122053.
[2] F. Khavari, M. Saidijam, M. Taheri, F. Nouri, *Mol Biol Rep* **2021**, *48*, 4757.
[3] M. Rizwan, G. Mujtaba, S. A. Memon, K. Lee, N. Rashid, *Renewable and Sustainable Energy Reviews* **2018**, *92*, 394.
[4] D. T. Tran, N. K. Nguyen, A. S. Yadav, A. Chuang, M. Burford, C. H. Ooi, K. R. Sreejith, N. T. Nguyen, *RSC Adv* **2024**, *14*, 15441.
[5] P. Bodenes, H. Y. Wang, T. H. Lee, H. Y. Chen, C. Y. Wang, *Biotechnol Biofuels* **2019**, *12*, 33.
[6] Y. J. Juang, J. S. Chang, *Biotechnol J* **2016**, *11*, 327.
[7] S. Han, Q. Zhang, X. Zhang, X. Liu, L. Lu, J. Wei, Y. Li, Y. Wang, G. Zheng, *Biosens Bioelectron* **2019**, *143*, 111597.
[8] D. T. Tran, A. S. Yadav, N. K. Nguyen, P. Singha, C. H. Ooi, N. T. Nguyen, *Small* **2023**, e2303435.
[9] Y. Yang, R. Dong, S. Zhang, J. Geng, F. Wang, S. Liu, L. Tao, W. Li, C. Chen, Z. Qian, *Sci Total Environ* **2022**, *816*, 151615.
[10] C. Castaldello, E. Sforza, E. Cimetta, T. Morosinotto, F. Bezzo, *Industrial & Engineering Chemistry Research* **2019**, *58*, 18036.
[11] A. Dewan, J. Kim, R. H. McLean, S. A. Vanapalli, M. N. Karim, *Biotechnol Bioeng* **2012**, *109*, 2987.
[12] Z. Yu, K. Geisler, T. Leontidou, R. E. B. Young, S. E. Vonlanthen, S. Purton, C. Abell, A. G. Smith, *Algal Res* **2021**, *56*, 102293.
[13] N. Shembekar, C. Chaipan, R. Utharala, C. A. Merten, *Lab Chip* **2016**, *16*, 1314.
[14] M. Soroor, M. Zabetian Targhi, S. A. Tabatabaei, *European Journal of Mechanics - B/Fluids* **2021**, *89*, 289.
[15] D. Zhang, L. Qiao, *Small Methods* **2024**, *8*, e2301179.
[16] A. S. Yadav, F. M. Galogahi, A. Vashi, D. T. Tran, G. S. Kijanka, H. Cha, K. R. Sreejith, N. T. Nguyen, *Biomed Microdevices* **2024**, *26*, 24.
[17] P. Zhang, A. M. Kaushik, K. Hsieh, S. Li, S. Lewis, K. E. Mach, J. C. Liao, K. C. Carroll, T. H. Wang, *Small Methods* **2022**, *6*, e2101254.
[18] J. R. O. Bianchi, L. G. de la Torre, A. L. R. Costa, *Foods* **2023**, *12*, 3385.
[19] F. M. Galogahi, M. Christie, A. S. Yadav, H. An, H. Stratton, N. T. Nguyen, *Analyst* **2023**, *148*, 4064.
[20] L. Zou, B. Huang, X. Zheng, H. Pan, Q. Zhang, W. Xie, Z. Zhao, X. Li, *Materials Chemistry and Physics* **2022**, *276*, 125384.
[21] M. Oveysi, M. A. Zaker, G. Peregrino, V. Bazargan, M. Marengo, *Microfluidics and Nanofluidics* **2023**, *27*, 45.
[22] L. Yu, Q. Sun, Y. Hui, A. Seth, N. Petrovsky, C. X. Zhao, *J Colloid Interface Sci* **2019**, *539*, 497.
[23] C. Zhang, R. Grossier, N. Candoni, S. Veesler, *Biomater Res* **2021**, *25*, 41.
[24] M. Chen, G. Bolognesi, G. T. Vladisavljevic, *Molecules* **2021**, *26*, 3752.
[25] H. Zhang, E. Tumarkin, R. M. A. Sullan, G. C. Walker, E. Kumacheva, *Macromolecular Rapid Communications* **2007**, *28*, 527.
[26] K. Enck, S. P. Rajan, J. Aleman, S. Castagno, E. Long, F. Khalil, A. R. Hall, E. C. Opara, *Ann Biomed Eng* **2020**, *48*, 1103.
[27] L. Liu, F. Wu, X. J. Ju, R. Xie, W. Wang, C. H. Niu, L. Y. Chu, *J Colloid Interface Sci* **2013**, *404*, 85.
[28] A. Sattari, S. Janfaza, M. Mashhadi Keshtiban, N. Tasnim, P. Hanafizadeh, M. Hoorfar, *ACS Omega* **2021**, *6*, 25964.
[29] H. Shieh, M. Saadatmand, M. Eskandari, D. Bastani, *Sci Rep* **2021**, *11*, 1565.
[30] Y. Liu, N. Tottori, T. Nisisako, *Sensors and Actuators B: Chemical* **2019**, *283*, 802.
[31] P. Agarwal, J. K. Choi, H. Huang, S. Zhao, J. Dumbleton, J. Li, X. He, *Part Part Syst Charact* **2015**, *32*, 809.
[32] F. M. Galogahi, A. Ansari, A. J. T. Teo, H. Cha, H. An, N. T. Nguyen, *Biomed Microdevices* **2022**, *24*, 40.
[33] L. Lin, C. K. Chung, *Micromachines (Basel)* **2021**, *12*, 1350.
[34] D. J. Collins, A. Neild, A. deMello, A. Q. Liu, Y. Ai, *Lab Chip* **2015**, *15*, 3439.
[35] J. Zhao, Q. Guo, W. Huang, T. Zhang, J. Wang, Y. Zhang, L. Huang, Y. Tang, *Polymers (Basel)* **2020**, *12*, 688.
[36] A. G. Hati, D. C. Bassett, J. M. Ribe, P. Sikorski, D. A. Weitz, B. T. Stokke, *Lab Chip* **2016**, *16*, 3718.
[37] D. H. Lee, C. Y. Bae, J. I. Han, J. K. Park, *Anal Chem* **2013**, *85*, 8749.
[38] T. Takahashi, *Molecules* **2019**, *24*, 4441.
[39] A. Xaaldi Kalhor, A. Movafeghi, A. D. Mohammadi-Nassab, E. Abedi, A. Bahrami, *Mar Pollut Bull* **2017**, *123*, 286.
[40] Y. Jeong, J. Irudayaraj, *Acta Biomater* **2023**, *158*, 203.
[41] A. Pannier, U. Soltmann, B. Soltmann, R. Altenburger, M. Schmitt-Jansen, *J Mater Chem B* **2014**, *2*, 7896.
[42] D. T. Tran, N. K. Nguyen, A. S. Yadav, A. Chuang, M. Burford, F. M. Galogahi, K. R. Sreejith, N. T. Nguyen, *Advanced Energy and Sustainability Research* **2024**, *5*, 2400112.
[43] G. Chan, D. J. Mooney, *Acta Biomater* **2013**, *9*, 9281.

Manuscript received: October 15, 2024
Revised manuscript received: January 7, 2025
Accepted manuscript online: February 9, 2025
Version of record online: ■■, ■■

RESEARCH ARTICLE

This study explores the use of droplet-based microfluidic technology combined with external gelation to produce calcium alginate hydrogel beads for encapsulating and cultivating microalgae *Chlorella vulgaris*. Beads crosslinked the with highest calcium ion concentration (1 g/mL) showed superior uniformity and stability, supporting steady microalgae growth over five days, highlighting their potential for controlled microalgae cultivation applications.

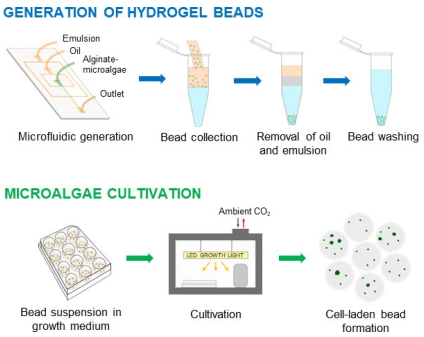

*D. Tuan Tran, F. Malekpour Galogahi, N.-K. Nguyen, U. Roshan, A. Singh Yadav, K. Rajan Sreejith, N.-T. Nguyen**

1 – 10

Microfluidic Generation of Calcium Alginate Hydrogel Beads using External Gelation for Microalgae Cultivation